194-Pos

Molecular Modelling Studies of Bovine and Camel Chymosin-κ-Casein Complexes

Jesper Sørensen[1], David S. Palmer[1], Anders U. Christensen[1], Leyla Celik[2], Karsten B. Qvist[3], Birgit H. Schiøtt[1].
[1]Aarhus University, Aarhus C, Denmark, [2]Yale University, New Haven, CT, USA, [3]Chr. Hansen, Hørsholm, Denmark.

We present computational studies of two homologous mammalian aspartic proteases (calf and camel chymosin) complexed with 16-residue fragments of their native peptide ligands (cow and camel κ-casein) and the cross-complexes. Using molecular docking calculations, homology modelling and molecular dynamics simulations, we compare the binding modes of the four systems. The complexes are of industrial interest because camel chymosin has recently been marketed as an alternative to bovine chymosin as an enzyme to clot milk in cheese manufacturing. The camel enzyme has been shown to have 70% higher clotting activity and only 20% of the unspecific protease activity for bovine κ-casein as compared to the bovine enzyme. Interestingly, bovine chymosin has a very low proteolytic rate for camel κ-casein. The models provide putative atomic coordinates for these complexes, for which there are no available crystallographic or NMR structures, and help to explain some existing experimental results.

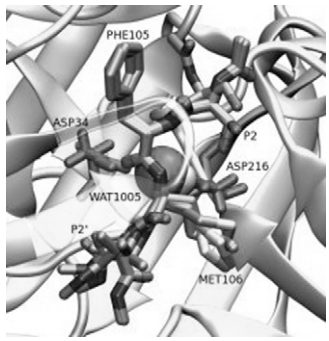

195-Pos

Changes in HIV-1 Protease-Inhibitor Interaction Due to Amino Acids Polymorphisms and Drug-Pressure Selected Mutations

Angelo M. Veloro, Mandy E. Blackburn, Jamie L. Kear, Xi Huang, Gail E. Fanucci.
University of Florida, Gainesville, FL, USA.

Both pulsed electron paramagnetic resonance (EPR) and 2D HSQC NMR are used to study HIV-1 protease-inhibitor binding by monitoring the changes in flaps conformation and amide chemical shifts. For all NMR and EPR experiments, here, we used an inactive (D25N) enzyme construct and nine FDA approved inhibitors. Results show that several inhibitors induce a closed flap conformation and cause significant splitting of the amide backbone chemical shifts due to a removal of the homodimer symmetry upon binding. Other inhibitors are found to interact more weakly with the protein, resulting in incomplete flap closures and perturbation of HSQC peaks due to chemical exchange. Qualitatively, both the pulsed EPR and NMR methods can discern different degrees of protease-inhibitor interactions, which we define as strong, moderate, and weak. The stability of each of the protease-inhibitor formed was determined by measuring the transition midpoint (Tm) with differential scanning calorimetry (DSC). Inhibitors classified as ''strong binders'' have higher Tm values. To determine changes in protease-inhibitor interaction with drug resistant constructs, we used the inactive sub-Saharan HIV-1 protease (8 amino acid polymorphisms), MDR769 (11 mutations) and V6 (8 mutations). Our pulsed EPR and NMR results show differences in inhibitor interactions in subtype C, MDR769 and V6 compared to subtype B.

196-Pos

Interactions Within the E2 Enzyme Cdc34-Ubiquitin Complex Are Transient

Donald E. Spratt, Anne C. Rintala-Dempsey, Kathryn R. Barber, Gary S. Shaw.
University of Western Ontario, London, ON, Canada.

The process of ubiquitylation involves the transfer of the small 76-residue protein ubiquitin (Ub) between a series of enzymes (E1, E2, E3) until it binds to a lysine residue of the substrate protein. When repeated several times, the E1-E2-E3 cascade forms a K48-linked polyubiquitin (poly-Ub) chain targeting the protein substrate for 26S proteasomal degradation. The E2 enzyme is the key protein in this cascade as it must recognize both the E1 and E3 enzymes, label the substrate, as well as form a covalent thiolester with Ub. Cdc34 is a class II E2 conjugating enzyme in the Ub-dependent degradation pathway of cell cycle proteins. It is comprised of a ~170 residue catalytic domain, common to all E2 enzymes, which contains the active site cysteine (C93). Two unique features of cdc34 are its acidic loop (residues 102-113) and acidic tail (residues 171-236), both of which are required to produce poly-Ub chains. However, the underlying mechanism that these regions have on chain assembly remains unclear. We have used NMR spectroscopy to study protein-protein interactions between cdc34 and Ub by using a stable covalent disulphide cdc34-Ub to mimic the thiolester complex. Chemical shift mapping was used to identify sites of non-covalent interactions in the cdc34-Ub to create a model of the complex. Competitive binding studies using free Ub or the cdc34 tail (residues 183-236) with cdc34-Ub indicate that transient non-covalent interactions exist between cdc34 and Ub. These studies provide the first detailed structural information to explain the unique mechanism used by cdc34 to promote poly-Ub chain assembly.

197-Pos

Binding of Small-Molecule Inhibitors To MAP Kinase ERK2, Studied with Resonance Energy Transfer (RET)

Kerrick Nevels, Paul Shapiro, Peter Butko.
University of Maryland School of Pharmacy, Baltimore, MD, USA.

The extracellular-signal-regulated kinase (ERK) proteins belong to the mitogen-activated protein kinase family. They participate in several important cell-signaling pathways. Unregulated, ERK2 is thought to mediate cell proliferation in many types of cancer. But because ERK also functions in many normal cell activities, inhibition selectivity is necessary for its use in cancer therapy: one needs to block only phosphorylation of those substrates that are involved in cell proliferation, while leaving phosphorylation of other substrates unaffected. Novel small-molecule compounds, which inhibit phosphorylation of selected substrates but do not compete with ATP for its binding site, have been previously identified by computer-aided drug design (CADD) and molecular-dynamics docking algorithms. Herein, we spectroscopically characterized selected compounds, and show that they can serve as resonance energy transfer (RET) acceptors for tryptophan: we determined the values of spectral overlap J between the compounds' absorption and ERK fluorescence, and of the Forster distance R_0 for the compound/tryptophan pairs. We then used RET to determine average distances between the bound compounds and the group of three tryptophans in ERK2, thus validating the CADD predictions of the compounds' binding sites. The problem of multiple but closely located donors (tryptophans) that pass the energy to the single acceptor (the bound compound) is discussed, as is the possibility of utilizing RET for mapping the inhibitor-binding sites on other kinases. The novel RET acceptors for tryptophan can conceivably be employed in studies of other protein/ligand systems with suitable spectroscopic properties.

198-Pos

Receptor Transactivation Measured in Live Cells Using Spatial Intensity Distribution Analysis (spida)

Antoine G. Godin[1], Jody L. Swift[1], Kim Doré[1], Mikhail Sergeev[1], Laure Freland[2], Yves De Koninck[3], Martin J. Beaulieu[3], Paul W. Wiseman[1].
[1]McGill, Montreal, QC, Canada, [2]Université Laval, Québec, QC, Canada, [3]Laval Université, Québec, QC, Canada.

Recent evidence suggests that signaling responses elicited by G-protein coupled receptors (GPCRs) are more complex than first believed. For instance, stimulation of several GPCRs leads to the transactivation of receptor tyrosine kinase (RTK) signaling pathways. Many groups have studied the role and mechanistic details of RTK-GPCR cross communication, using standard biochemical methods. While these studies have helped to elucidate possible intermediates involved in this complex network, the diversity of cell types and receptors used has often lead to conflicting results and provided little quantitative information.

We present a quantitative measurement of RTK transactivation, using spatial intensity distribution analysis (SpIDA). Employing confocal microscopy, spatial intensity histograms are fit using super-Poissonian distributions, yielding molecular parameters such as density and particle quantal brightness. SpIDA provides measurement of particle densities and oligomerization states of receptors using single images as input. Thus processes such as transactivation, which results in changes in the oligomerization state, can be monitored. CHO-K1 cells expressing EGFR-GFP were transfected with various GPCRs including β2-arrestin, neurokinin1, angeotensin and dopamine receptors. We monitored the relative distribution of monomeric and dimeric EGFR in response to GPCR stimulation and obtained dose response curves for different EGFR-GFP:GPCR interactions.

To confirm our findings, similar dose response curves were obtained using FLIM-FRET data and negative controls were also measured when activation or transactivation was blocked with a variety of biochemical agents including Rab5 and AG1478.

By fitting dose response curves to standard models, key parameters such as D50, and Dmax were obtained. To show that those results were not biased by either cell type choice or overexpression, we studied transactivation in situ in primary

cell cultures from mouse brain neurons and quantified dimerization of the BDNF receptor due to both direct and trans-activation via dopamine.

199-Pos

Why Is α4β2 Nachr More Sensitive to Volatile Anesthetics Than α7 Nachr?

David D. Mowrey, Lu T. Liu, Dan Willenbring, Esmael J. Haddadian, Yan Xu, Pei Tang.
University of Pittsburgh, Pittsburgh, PA, USA.

Two subtypes of neuronal nicotinic acetylcholine receptors (nAChRs) show different functional sensitivities to volatile anesthetics: the α4β2 nAChR is hypersensitive while the α7 nAChR is insensitive. To understand why these homologous proteins have different functional responses to volatile anesthetics, we performed multiple sets of 20-ns molecular dynamics (MD) simulations on the closed- and open-channel α7 in the absence and presence of halothane, and compared the results with those from a similar study on the α4β2 nAChR (Liu, et al. 2009). The details about construction of receptor structural models were published (Haddadian, et al. 2008). Initial halothane docking and subsequent MD simulations revealed several halothane-binding sites in α7. Consistent with observations from α4β2, free energy perturbation calculations showed that halothane had higher binding affinity in the closed- than the open-channel; α7 and α4β2 had a comparable number of high affinity sites. GNM analysis showed that halothane induced profound changes in correlated domain motion of the open-channel α4β2, especially between the Cys-loop and the TM2-TM3 linker, but had a negligible impact to the motion of the α7. Salt bridges between these loops in the β2 subunit may be responsible for the aforementioned observation. Flexibility of several key loops in the open-channel α4β2 changed considerably in the presence of halothane, but the same loops in the open-channel α7 showed little change. Taken together, our results suggest that halothane binding in nAChRs may be necessary, but not sufficient to produce essential dynamical changes that alter protein functions. Although α7 and α4β2 are homologous, specific residues in key loops may make α4β2 more susceptible to volatile anesthetics while α7 unaffected. Supported by NIH (R01GM66358, R01GM56257, and T32GM075770) and NCSA through the PSC.

200-Pos

Conformational Docking of Multiple Toxins Against Kv1-Channels Highlight Key Motifs For Selectivity

Po-chia Chen, Serdar Kuyucak.
University of Sydney, University of Sydney, Australia.

Scorpions and other venomous predators are known to disable their prey via injection of peptides, which interfere with ion channels involved in neural signalling. These peptides are both highly specific blockers and potential scaffolds for toxin-based therapeutics of diseases such as multiple sclerosis, thus attracting continual research.

The key functional motif of toxins against Kv-channels is a dyad composed of a pore blocking lysine and a nearby aromatic residue. Several groups have also proposed the presence of 'basic ring' motifs to explain extreme selectivity for channel subtypes in several toxins. Since experimental validation of specificity is difficult due to numerous toxin-channel combinations, we sought to create a comprehensive database in-silico via the program HADDOCK. The Kv1.2 structure was used to construct its homologues Kv1.1 and Kv1.3, and submitted in blind-docking protocols versus ~30 toxins to isolate consensus binding modes. We find that all toxins share a small number of binding modes, classified by the identity of the residue inserted into the channel pore. HADDOCK outputs a near-native mode as the top-ranked pose in over 50% of runs, or ~90% if the top 5 is considered. Identification of other modes, e.g. associated with KCa2-channel binding, suggests that some toxins may bind to multiple targets. We also find peripheral residues have roles interacting with the channel S5P loop - confirming that the basic ring acts to discriminate Kv1 channels versus other potassium channels.

At the time of writing, we are in the process of completing the database with a hypothesis that Kv1-subtype selectivity arises from: (a) exact surface/hydrophobic matching, and (b) charge content and positioning. We ultimately aim to find an optimal scaffold for Kv1.3 and extension towards other K+-channel subtypes as more structures are published.

201-Pos

Theoretical Models of the Biological Catch-Bond

Yuriy Pereverzev, **Oleg Prezhdo.**
University of Washington, Seattle, WA, USA.

The biological catch-bond is a fascinating and counterintuitive phenomenon, which was predicted theoretically 30 years ago. Recently, this predicted behavior has been observed in a number of protein receptor-ligand complexes. When an external force is applied to a catch-bond in an attempt to break it, either *in vivo* or *in vitro*, the bond resists breaking and becomes stronger instead. This is in contrast to ordinary slip-bonds which represent the vast majority of biological and chemical bonds and which dissociate faster when subjected to a force. This report focuses on the fundamental properties of catch-bonds and analyzes the simplest physical-chemical models to explain the experimental data. The simplicity of the theoretical treatment leads to analytic expressions for bond lifetime, concise universal representations of the experimental data, and explicit conditions required for catch-binding.

Three different model of the biological catch-bond will be discussed, including the two pathway, deformation and allosteric models. Catch-binding is a consequence of a complex potential energy landscape in a biological receptor-ligand bond. Bond lifetime can increase with force, if this force prevents dissociation through a native pathway and instead drives the system over a higher energy barrier. The lifetime can also increase if the conformations of proteins in the complex are altered by the force in a way that strengthens receptor-ligand interaction. Such bond deformation can be associated with an allosteric effect, in which a conformational change at one end of the protein propagates to the binding site located at the other end. Both experiment and simulation indicate that catch-binding is accompanied by large-scale domain opening in the receptor protein. The models are used to describe catch-binding in P-selectin/PSGL-1, FimH/mannose, actin/myosin and integrin/fibronectin complexes.

O. V. Prezhdo, Y. V. Pereverzev, ''Theoretical aspects of the biological catch-bond'', *Acc. Chem. Res.*, **42**, 693 (2009).

202-Pos

Correlation Between Functionality and Biochemical Properties in Biotin Protein Ligases

Kyle Daniels, Dorothy Beckett.
University of Maryland, College Park, MD, USA.

Biotin protein ligases are a family of enzymes that catalyze biotin linkage to biotin-dependent carboxylases. In microorganisms these enzymes are functionally divided into two classes including the monofunctional class that only catalyzes biotin addition and the bifunctional class that also binds to DNA to regulate transcription. Biochemical and biophysical studies of the bifunctional Escherichia coli ligase suggest that several properties of the enzyme have evolved to support its additional regulatory role. These properties include the order of binding of multiple substrates and linkage between oligomeric state and ligand binding.

In order to test the hypothesized relationship between bifunctionality and enzymatic properties in ligases, we have carried out studies of monofunctional ligase from Pyrococcus horikoshii. Sedimentation equilibrium measurements to determine the effect of ligand binding on oligomerization indicate that the enzyme exists as a dimer regardless of liganded state. Isothermal titration calorimetry and fluorescence spectroscopy measurements of substrate binding indicate that, unlike in the E. coli enzyme, substrate binding is not ordered. Finally, thermodynamic signatures of ligand binding to the monofunctional enzyme differ significantly from those measured for the bifunctional enzyme. Combined studies of the bifunctional and monofunctional biotin ligases indicate a link between the functionality of these enzymes and their detailed biochemical characteristics.

203-Pos

Remote Regions Involved in Phosphoenolpyruvate Binding to Lactobacillus Delbreuckii Phosphofructokinase

Scarlett A. Blair, Gregory D. Reinhart.
Texas A&M Univ, College Station, TX, USA.

Phosphofructokinase from Lactobacillus delbrueckii subspecies bulgaricus (LbPFK), unlike that from Thermus thermophilus (TtPFK) and Bacillus stearothermophilus (BsPFK), exhibits weak binding affinity for the allosteric inhibitor phospho(enol)pyruvate (PEP). LbPFK has 57% sequence identity, with 75% similarity, to BsPFK and 48% identity, with 65% similarity, to TtPFK. A comparison of crystal structures between apo-LbPFK and apo-BsPFK indicates an overall conservation in structure except for the allosteric binding site. The two regions within the allosteric binding site which differ between LbPFK and other PFKs include the end of an a-helix containing residues 55-59 and a loop containing residues 211-215. Individual mutations were made in both of these regions to the corresponding residues from either TtPFK or BsPFK, with no enhancement in PEP binding. Therefore, chimeric substitutions were introduced into LbPFK in which all the residues in these regions were replaced with those from TtPFK, since TtPFK binds PEP 18,000-fold tighter when compared to LbPFK. Tt(52-61)/LbPFK and Tt(206-218)/LbPFK resulted in no enhancement in PEP binding when compared to LbPFK. They were also combined to form Tt(52-61,206-218)/LbPFK, which again exhibits similar PEP binding to LbPFK. These results indicate that the weak PEP binding in LbPFK cannot be explained as due solely to the residues which directly interact with the ligand upon binding. Another region of interest is the a-helix